# System Level Evaluation of UL and DL Interference in OFDMA Mobile Broadband Networks

David Halls, Andrew Nix and Mark Beach

Centre for Communications Research,
University of Bristol, Bristol, United Kingdom.
Email: {David.Halls.03, Andy.Nix, M.A.Beach}@bristol.ac.uk

*Abstract* — **This paper presents results from a novel OFDMA multi-cell mobile broadband system level simulator. The tool is used to statistically characterize uplink and downlink inter-cell interference. Without suitable interference management, multi-billion dollar networks can collapse under the strain of heavy traffic loads. Fully loaded interference studies cannot be performed on the network until it has been fully deployed. As such, interference analysis and management must be accurately performed pre-deployment using detailed network simulators. System level simulation is a highly computationally intensive procedure. This paper discusses the simulator architecture (and steps taken to reduce computational complexity) and then demonstrates the impact of inter-cell interference in OFDMA networks. In an interference limited scenario the results demonstrate that it is the frame-to-frame fluctuations in interference, and not the received signal level, that dominate inaccuracies in the Channel Quality Index (CQI) prediction. CQI is used in the fast link-adaptation process to select the MCS mode for each user on a frame-by-frame basis. Results show that incorrect Modulation and Coding Scheme (MCS) modes are chosen up to 40% of the time when the CQI is delayed by 3 frames and the user is interference limited. Perfect MCS selection is then shown to improve user throughput by up to 50%.**

***Keywords- mobile broadband; interference characterization; cellular; MIMO; WiMAX; system level evaulation.***

## I. INTRODUCTION

This paper evaluates the inter-cell interference performance of a Wave-2 MIMO mobile WiMAX system. The simulator is based on the IEEE 802.16m amendment, which provides the basis for next generation mobile WiMAX systems. WiMAX uses scalable OFDMA in the radio access network [1]. In order to achieve the spectral efficiency and per-sector throughput required by voice, data and media applications, WiMAX makes use of Adaptive Modulation and Coding (AMC) and Multiple Input Multiple Output (MIMO) antenna processing. To achieve high user capacity it is necessary to perform well at high traffic load. Unless deployed correctly, such networks can collapse under heavy load due to self-interference. The commercial success of mobile broadband networks is dependent on accurate interference characterization and management. It is therefore critical, pre-deployment, to accurately evaluate system level performance in the presence of uplink (UL) and downlink (DL) interference. It is also important to understand how interference is affected by the radio environment and different propagation scenarios. Due to real-world difficulties in loading a network and varying the propagation scenarios during drive tests, the comprehensive interference characterization of multi-cellular systems cannot easily be achieved in practice. Heavy UL traffic loads are particularly difficult to engineer in controlled tests. This makes accurate interference characterization via simulation an absolute necessity prior to network deployment.

Interference arises in the form of inter-cell and intra-cell interference. Whereas intra-cell interference is relatively easy to manage by means of orthogonal frequencies and scheduling strategies, inter-cell interference is problematic and remains a key issue in OFDMA based mobile cellular networks. This is because in broadband wireless networks, sector frequencies are reused in adjacent cells to improve spectral efficiency. The problem is particularly acute at the cell boundaries, where wanted signal powers are weak and interfering signal power strong; this results in reduced user throughput. Characterization of inter-cell interference for OFDMA networks is not well addressed in the literature – particularly on the UL. This is mainly due to the complexity of simulating a vast quantity of links simultaneously, and over a statistically significant time period.

## II. BACKGROUND

In order to characterize interference accurately in a mobile broadband network it is necessary to model a multi-cell environment that implements a realistic cellular reuse factor, uses full size frame structures over many frames, and implements subcarrier allocation and packet scheduling.

As discussed in [2], the link budget constraint on the UL necessitates the need for smaller cell sizes. The use of small site-to-site distances makes for highly interference limited systems. In order to analyze UL interference, knowledge is required of the desired MS location as well as the relative locations of all other interfering MSs. All the necessary fading channels must then be computed for the scheduled users in each frame. The authors in [3] considered interference randomization on both the UL and DL of a WiMAX system However, they failed to implement a full system level simulator. The authors in [4] examined UL performance using a proprietary simulator (SHINE). This paper also explores a range of complexity reduction techniques. This is vital in order to create a simulator that can accurately characterize interference in a timely manner.

The work of David Halls was supported in part by the Engineering and Physics Research Council (EPSRC) of UK and in part by Motorola UK.

Complexity can be reduced by simplifying the computation of interference. In [5] the subcarriers from adjacent cells are simply scaled by a 'loading factor' to mimic the loading process, rather than accurately scheduling users and computing the resulting UL and DL interference. Although other simulators make use of correlated fast fading models, they commonly use random [5] or uniform [6] MS locations between drops, and uncorrelated (spatially) log normal shadowing [6]. Although they may implement AMC, the results are unrealistic since they assume perfect and instantaneous channel knowledge.

To aid complexity reduction, many simulators use a much reduced frame size. In [7] the authors use just 48 sub-carriers and 6 sub-bands. Very few papers use the full number of subchannels and slots per frame. In [8] the full frame structure is implemented as per [9], however they do not consider power control, scheduling, or UL traffic.

Although many commercial network simulators exist, such as OpNet and QualNet, these tend to provide weak physical layer support. QualNet uses bit error rate (BER) look up tables that already include fast-fading effects. Accurate simulators need to work with instantaneous performance in a fading channel, not the expected performance averaged over the fading processes.

In this paper, a system-level simulation framework is presented that allows the performance of a MIMO based Wave-2 mobile WiMAX system to be derived. The simulator closely follows the Evaluation Methodology Document (EMD) [9] in terms of: system parameters (such as transmit powers and antenna patterns) and simulation parameters (cell configuration, frame structure, traffic model, and MIMO). Enhancements above and beyond the EMD baseline are highlighted as they are introduced in the paper.

Our system implements AMC, MIMO with Adaptive MIMO Switching (AMS), alongside Dynamic Transmit Power Control (DTPC) on the UL [10]. It schedules and models all users in both the reference and interfering sectors. Unlike other reported works, a fully temporally and spatially correlated model is used for fast fading and shadowing [11]. The simulator comprehensively models the mobility of users (indoor, outdoor pedestrian and vehicular) to allow the simulation of fast link adaptation. The bespoke spatial channel model includes a realistic range of K-factors, RMS delay spreads and angular spreads.

A PHY layer abstraction technique known as Received Bit Mutual Information (RBIR) is used to predict instantaneous BLER at every instant. The abstraction model has been validated against link-level results from our own link-layer simulator. This in turn has been validated against results obtained from carrier-class mobile WiMAX equipment. Our novel AMC/AMS algorithm uses the 'effective' SINR (ESINR), as its Channel Quality Index, to calculate the optimal burst profile (MCS and MIMO mode) for each user in order to maximize throughput for a given BER requirement. This ESINR is calculated from all the subcarriers allocated to that user using the RBIR technique. We then simulate the full frame structure including UL and DL. We implement the mandatory PUSC subcarrier permutation scheme and a packet scheduler. The packet scheduler runs using a proprietary proportional fair (PF) algorithm. It also supports all of the WiMAX traffic classes by providing strict prioritization. As per the EMD baseline our simulator:

- Models a tri-sector multi-cell environment with micro and macro scenarios,
- Models full size frame structures for UL/DL with PUSC,
- Uses correlated fast fading,
- Implements a full range of MIMO modes,
- Uses an accurate and validated PHY abstraction model.

In addition our simulator:

- Exhaustively models all interferers,
- Uses sophisticated correlated shadowing model with validated autocorrelation function (ACF) and continuity of user mobility between frames,
- Implements AMS/AMC with channel feedback delay,
- Implements a proprietary PF scheduler with service class prioritization,
- Implements DTPC.

## III. Simulator Description

### A. System Overview

Only SISO results are shown in this paper. We also assume perfect channel estimation and synchronization. Equal power per subcarrier on the DL is applied. A full-buffer traffic model is assumed with best effort (BE) flows, since these most clearly highlight the impact of interference on fast link-adaptation performance. Tables I and II summarize the key system and simulation parameters. In mobile WiMAX the minimum resource unit is a 'slot'. This is 1 subchannel x 2 OFDM symbols on the DL and 1 subchannel x 3 OFDM symbols on the UL. Each slot is dynamically assigned to an MS using the packet scheduler.

TABLE I. System Parameters

| Parameters | | Value |
|---|---|---|
| BS | Transmit power | 43dBm |
| | Antenna height | 32m |
| | Antenna gain (boresight) | 17dBi |
| | 3dB beamwidth | 70° |
| | Front-to-back power ratio | 20dB |
| | Number of antennas (Rx and Tx) | 2 |
| | Antenna spacing | 4λ |
| | Noise figure | 4dB |
| | Cable loss | 2dB |
| MS | Transmit power | 23dBm |
| | Antenna height | 1.5m |
| | Antenna gain (boresight) | 0dBi |
| | Antenna pattern | Omni |
| | Number of antennas (Rx and Tx) | 2 |
| | Antenna spacing | λ/2 |
| | Noise figure | 7dB |
| | Cable loss | 0dB |

TABLE II. LINK AND SYSTEM SIMULATOR PARAMETERS

| Parameters | Value |
|---|---|
| Carrier frequency | 2.5GHz |
| Transmission bandwidth | 5MHz |
| FFT size | 512 |
| Cellular configuration | Hexagonal cell/2 tiers/7 cells |
| Antenna patterns | 3 sectors |
| Frame length | 5ms (48 OFDMA symbols) |
| Control symbols | 11 (1 preamble, 1 transceiver turnaround gap, 6 DL, 3 UL) |
| Data symbols | 28 DL/9 UL |
| Subchannels | 15 DL/17 UL |
| MCS Modes | QPSK 1/2, 3/4, 16QAM 1/2 2/3, 64QAM 2/3, 3/4 |
| AMC BER threshold | $10^{-6}$ |
| MCS feedback delay | 0, 1 and 3 frames |
| Frequency reuse factor | 1/3 |
| Antenna scheme | SISO |
| Scheduling algorithm | Round robin, (1 subchannel/partition) |
| Mobility | Pedestrian (3kmph) |
| Penetration loss | 10dB |
| Traffic class | Best Effort |
| Traffic model | Full buffer |
| Shadowing SD | 8dB |
| De-correlation distance | 50m |
| Power Control $P_{nom}$ | 21.4dB |
| Spatial Channel Model | CDL using spatial correlation |
| Pathloss model | COST 231 Hata |

## B. *Link-Layer Simulator Description*

The link-level simulator is fully described in [12] and the results have been fully validated against carrier-class equipment. Figure 1 shows the BLER vs. SINR results from the simulator in an AWGN channel. These are used later link-to-system mapping. A block is a single WiMAX 'slot'.

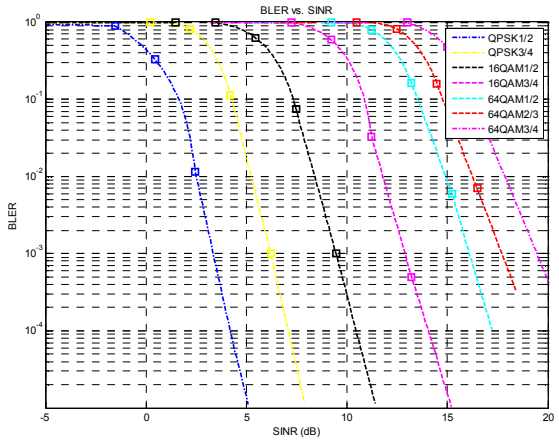


Figure 1. Block Error Rate under AWGN channel

## C. *Spatial Channel Model (SCM)*

A correlation-based Cluster Delay Line model is used with parameters taken from the 'Urban Macrocell' scenario (Table III). The full power delay profile is provided in [9].

TABLE III. CHANNEL MODEL PARAMETERS

| Scenario | Cell Radius | (N)LOS | AS (BS,MS) |
|---|---|---|---|
| Urban Macrocell | 500m | NLOS | 2°, 15° |

## D. *Pathloss, Antenna Gain and Shadowing*

BS and MS heights of 32m and 1.5m respectively are used in the modified COST 231 Hata path loss model ('Urban Macro cell') shown in (1), and defined in [9].

$$PL[dB] = 35.2 + 35\log_{10}(d) + 26\log_{10}(f/2) \qquad (1)$$

In (1) $d$ is defined in meters and represents the BS-MS separation distance. At the BS a Uniform Linear Array (ULA) is assumed with an antenna pattern as defined in [9]. The MSs are assumed to have omni-directional antenna patterns.

We implement a spatially correlated shadowing model as proposed in [11]. This is used to generate the shadowing values for the BS-MS links. The parameters are summarized in Table IV.

TABLE IV. SHADOWING PARAMETERS

| Parameter | Value |
|---|---|
| Shadowing SD | 8dB |
| Decorrelation distance | 50m |
| Number of sinusoids [11] | 500 |
| Frequency resolution [11] | 0.002 |
| Spatial resolution [11] | 0.5m |
| Waveform table size [11] | 1000 |

## E. *Link-to-System Mapping (PHY Abstraction)*

To simplify the interface between the link and system level simulations, whilst still modeling dynamic system behavior, a technique known as Effective SINR Mapping (ESM) can be used. This compresses the SINR (per subcarrier) vector into a single ESINR. Various ESM approaches are described in the literature, including Logarithmic ESM (LESM), mean instantaneous Capacity ESM (CESM), Exponential ESM (EESM) and Mutual Information ESM (MIESM). In this work the MIESM approach is applied, since unlike the other techniques, it achieves accuracy without the need for adjustment factors. The technique is described fully in [13].

The PHY abstraction model predicts the BLER for a given channel realization across the allocated OFDM subcarriers. In the SISO case, the post-processing SINR per subcarrier $n$, for user zero, may be expressed as

$$SINR^{(0)}(n) = \frac{P_{tx}^{(0)} P_{loss}^{(0)} \left|H^{(0)}(n)\right|^2}{\sigma^2 + \sum_{j=1}^{N_I} P_{tx}^{(j)} P_{loss}^{(j)} \left|H^{(j)}(n)\right|^2} \qquad (2)$$

where $j$ represents the interferer, $N_I$ represents the total number of interferers and $P_{loss}^{(j)}$ is the distance dependent path loss including shadowing. The Symbol Information (SI) for each of these subcarriers is then calculated. These values are averaged and normalized to find the RBIR. This is then mapped to an ESINR and this is mapped to a BLER using the non-faded SINR-to-BLER curves obtained from the link-level simulation (Figure 1). This technique has been exhaustively validated against our link-level simulator.

### F. Simulator Complexity

For every DL slot, the link between all of the users in the central cell and all of the BSs must be calculated (over all subcarriers). On the UL, the link between all of the MSs in the surrounding cells and the central BS is required. Channel information for 107,520 links is required to compute a single time slot. This is in addition to performing the permutation, link adaptation and scheduling algorithms. In order to reduce complexity, the channel is assumed to remain stationary over a 'slot'. Only 512 subcarriers are used and the analysis is limited to the 7 central cells. It is shown in [14] that the second tier of interferers can be ignored. In this paper, statistics are only collected for the central cell based on 5 active users in each of the 3 sectors. Use of the PHY layer abstraction approach is crucial. In order to further reduce computation time, the channel responses are calculated offline. The simulator is written in C++ and makes use of bespoke shared libraries coded in Matlab.

## IV. RESULTS

### A. Link Budget

Results will be given assuming 1) no PUSC permutation, 2) PUSC permutation with a common PermBase at all BSs, and 3) PUSC permutation with different PermBase values at each BS.

TABLE V. DL MEAN SNR AND SIR VALUES

| | | 0.0 | 0.1 | 1 | 1.1 | 1.2 | 1.3 | 1.4 | 2.0 |
|---|---|---|---|---|---|---|---|---|---|
| **No Perm** | **SNR** | 44.9 | 44.5 | 34.9 | 45.0 | 51.1 | 31.0 | 39.7 | 32.2 |
| | **SIR** | 38.0 | 37.0 | 35.0 | 41.3 | 51.6 | 23.8 | 38.3 | 12.8 |
| **Fixed PB** | **SNR** | 44.3 | 43.0 | 33.8 | 43.6 | 51.1 | 30.1 | 39.4 | 31.5 |
| | **SIR** | 39.3 | 36.4 | 33.8 | 39.9 | 52.0 | 22.9 | 36.9 | 11.9 |
| **Full PUSC** | **SNR** | 44.3 | 43.0 | 33.8 | 43.6 | 51.1 | 30.2 | 39.4 | 31.6 |
| | **SIR** | 39.4 | 36.5 | 33.7 | 39.9 | 52.0 | 23.0 | 36.8 | 12.0 |

TABLE VI. UL MEAN SNR AND SIR VALUES

| | | 0.0 | 0.1 | 1 | 1.1 | 1.2 | 1.3 | 1.4 | 2.0 |
|---|---|---|---|---|---|---|---|---|---|
| **No Perm** | **SNR** | 20.0 | 23.3 | 33.0 | 3.8 | 32.9 | -5.8 | 34.5 | 5.4 |
| | **SIR** | 27.2 | 24.0 | 25.3 | 3.7 | 38.8 | -0.7 | 31.3 | 2.6 |
| **Fixed PB** | **SNR** | 19.3 | 21.7 | 32.1 | 2.5 | 32.4 | -6.3 | 33.6 | 4.8 |
| | **SIR** | 28.3 | 23.5 | 24.5 | 2.2 | 38.5 | -1.6 | 30.5 | 1.8 |
| **Full PUSC** | **SNR** | 19.3 | 21.7 | 32.1 | 2.4 | 32.6 | -6.1 | 33.6 | 4.8 |
| | SIR | 18.8 | 23.6 | 33 | -0.8 | 30.7 | -6.9 | 33.8 | 5.4 |

The PermBase allocated to each BS controls its PUSC permutation sequence. Tables V and VI show the mean slot-averaged SNR and SIR values for 8 users over all time slots (denoted *sector.MS*) in all three cases for both the UL and DL. The slot-averaged value is the mean across all of the subcarriers the allocated slot. Other users are not shown for the sake of brevity. Each MS remains well within one coherence distance window. From these results we can deduce that on the DL, all of the users are interference limited, i.e. the mean SIR is significantly below the mean SNR. However, for our link budgets, only a subset of UL users are interference limited (e.g. MS 1.0). This is because although they achieve large sub-channelization gains (up to 12dB), the UL runs with approximately 20dB less transmit power. The exact value depends on the DTPC algorithm.

### B. Signal and Interference Variability

Tables VII and VIII show the variance of the slot averaged SNR and SIR for the same set of users as above. From these results it is clear that the variance of the SIR is significantly greater than that of the SNR in *all* cases.

TABLE VII. DL SNR AND SIR VARIANCE VALUES

| | | 0.0 | 0.1 | 1 | 1.1 | 1.2 | 1.3 | 1.4 | 2.0 |
|---|---|---|---|---|---|---|---|---|---|
| **No Perm** | **SNR** | 28.0 | 28.4 | 22.0 | 28.2 | 29.2 | 27.8 | 25.9 | 28.3 |
| | **SIR** | 31.4 | 43.1 | 50.9 | 54.8 | 58.6 | 54.6 | 57.2 | 66.0 |
| **Fixed PB** | **SNR** | 8.4 | 10.6 | 8.7 | 9.4 | 10.4 | 11.0 | 13.0 | 10.7 |
| | **SIR** | 41.8 | 40.9 | 36.5 | 34.3 | 40.5 | 37.5 | 36.5 | 43.6 |
| **Full PUSC** | **SNR** | 8.7 | 8.4 | 8.9 | 9.2 | 10.4 | 11.2 | 12.7 | 11.0 |
| | **SIR** | 42.5 | 40.0 | 35.8 | 34.2 | 40.6 | 38.0 | 35.7 | 44.9 |

TABLE VIII. UL SNR AND SIR VARIANCE VALUES

| | | 0.0 | 0.1 | 1 | 1.1 | 1.2 | 1.3 | 1.4 | 2.0 |
|---|---|---|---|---|---|---|---|---|---|
| **No Perm** | **SNR** | 32.1 | 29.7 | 25.7 | 25.6 | 25.6 | 24.4 | 27.2 | 22.2 |
| | **SIR** | 36.8 | 42.2 | 54.1 | 54.7 | 52.8 | 54.6 | 57.4 | 45.8 |
| **Fixed PB** | **SNR** | 7.9 | 8.4 | 9.5 | 9.5 | 10 | 7 | 9.2 | 9 |
| | **SIR** | 38.8 | 40.1 | 39.5 | 32.6 | 37.2 | 33.2 | 42.9 | 30.6 |
| **Full PUSC** | **SNR** | 7.8 | 8.4 | 9.4 | 10.7 | 9.8 | 8.4 | 9.1 | 9.1 |
| | **SIR** | 12.4 | 12.6 | 7.6 | 17.9 | 18.3 | 13.7 | 14.8 | 13 |

The use of subcarrier permutation significantly reduces the variance of both the SIR and SNR. The use of a varying PermBase does not affect the SNR variance. Furthermore, it does not reduce the variance of the DL SIR. As the BS transmits with equal power on all subcarriers within the interfering sector, the SIR is not affected statistically by the PermBase of the interfering BSs.

### C. Impact of Variability on MCS Choice

In the simulator, fast link-adaptation operates by collecting the CQI per MS in the form of the ESINR over all subcarriers allocated to that MS in a reference frame. The algorithm uses this to predict the highest order MCS mode that could be supported by each MS whilst maintaining a BER $< 10^{-6}$. The simulator was run with the following assumptions: a) zero frame delay (i.e. perfect per-frame CQI knowledge), b) 1-frame feedback delay, and c) 3-frame feedback delay (as per the EMD).

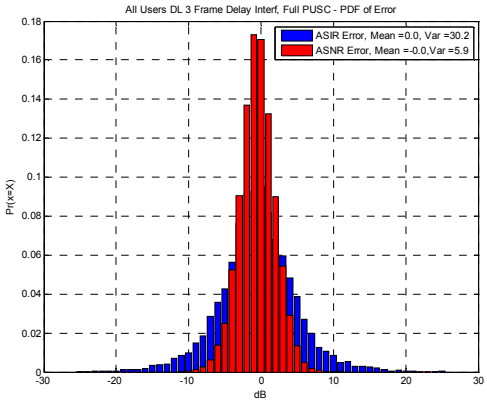


Figure 2. PDF ASNR and ASIR error for all DL users

The SIR, SNR and SINR values averaged over all of a user's allocated subcarriers in a frame are now denoted by ASIR, ASNR and ASINR respectively. These are distinct from the 'effective' values which have upper and lower bounds specific to each MCS mode thus making them inappropriate for some types of post processing. Figure 2 shows the PDF of the ASNR and ASIR error (i.e. the difference between the current and delayed frame). Results are shown for all DL users with full PUSC (i.e. a varying PermBase) and a feedback delay of 3 frames.

Mode selection is based on the CQI from the delayed frame so these SNR and SIR will translate to ESINR errors,

and these will produce MCS mode choice errors. If the ESINR in the scheduled frame is better than that predicted by the AMC algorithm, using delayed CQI information, then the scheduler MCS mode will be too low and network capacity will be lost. If the opposite is true, then the scheduled MCS mode will be too high and this will lead to high BLER. It is not surprising that delayed CQI information leads to these types of errors. However, we can see from the figure that the variance of the ASIR error is significantly higher than that of the ASNR error (and is even higher without PUSC). This leads us to conclude that in the interference limited case, it is the SIR variance and not the SNR variance that will dominate AMC performance.

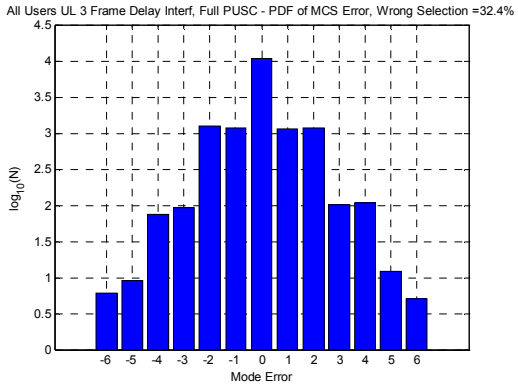


Figure 3. UL MCS selection error, full PUSC and 3-frame delay

Figure 3 shows the error statistics in the MCS mode choice for the case of 3-frame feedback delay for UL-PUSC. Positive errors imply the user's actual ESINR was higher than predicted and hence a higher MCS mode could have been used. Negative errors indicate the opposite. The wrong MCS mode was chosen for 32.4% of all UL users' frames. In the UL case, there are more positive errors than negative. This is because the MSs are often running in low modes so the error can not always be negative. Tables IX and X summarize the results for MCS usage error. The MCS selection error increases with CQI feedback delay. The use of PUSC is seen to reduce the mode selection error. On the UL the use of a varying PermBase further reduces the observed error variance.

The simulator was also run under the assumption of perfectly orthogonal interference. In this case, the ASINR error variance in each of the above cases equals the ASNR variance. Where this equates to a reduction in ASINR error – i.e. in interference-limited cases - the ESINR error falls and the MCS error falls correspondingly. For example; in the full PUSC DL case for all users, with a 3-frame CQI delay, the incorrect MCS mode usage ratio falls from 24% to 9.3%. The variance also falls, from 1.2 to 0.2, which shows that the severity of error reduces dramatically, as well as the occurrence. As the majority of full UL-PUSC users are not interference limited, when we remove interference the ASINR error variance only falls by 0.7dB, and the MCS error falls from 33.9% to 32%. However, for the interference-limited UL MS 1.0, the MCS error falls from 22.7% to 9.1%.

TABLE IX. DL SUB-FRAME MCS ERROR RESULTS

| Delay (Frame) | Perm | ASIR dB Err Var (dB) | ASNR Err Var (dB) | ASINR Err Var (dB) | ESINR Err Var (dB) | Incorrect MCS (%) |
|---|---|---|---|---|---|---|
| b) 1 | 1) | 9.1 | 4 | 5.7 | 3.5 | 15.4 |
| | 2) | 6.4 | 1 | 2.9 | 2.1 | 13.5 |
| | 3) | 6.3 | 1 | 2.9 | 2.2 | 13.5 |
| c) 3 | 1) | 44.5 | 21.6 | 32.4 | 16.6 | 25.7 |
| | 2) | 30.4 | 6.1 | 17.7 | 9.0 | 23.9 |
| | 3) | 30.2 | 5.9 | 17.6 | 9.1 | 24 |

TABLE X. UL SUB-FRAME MCS ERROR RESULTS

| Delay (Frame) | Perm | ASIR Err Var (dB) | ASNR Err Var (dB) | ASINR Err Var (dB) | ESINR Err Var (dB) | Incorrect MCS (%) |
|---|---|---|---|---|---|---|
| b) 1 | 1) | 9.2 | 4.1 | 4.4 | 3.5 | 22.2 |
| | 2) | 6.5 | 1.2 | 1.6 | 1.6 | 19.8 |
| | 3) | 1.7 | 1.2 | 1.3 | 1.3 | 17.6 |
| c) 3 | 1) | 45.0 | 21.9 | 24.4 | 17.8 | 38.1 |
| | 2) | 30.6 | 6.3 | 9 | 7.4 | 35.9 |
| | 3) | 9.8 | 6.3 | 7 | 5.9 | 33.9 |

### *D. Impact of MCS choice on Throughput*

MCS mode selection errors cause a reduction in user throughput. For DL MS 2.0 (interference limited) a CQI delayed by 3 frames results in an MCS error for 39.9% of frames. This leads to a reduction in the throughput over 1000 frames from 147 to 104kbps (29%). Figure 4 shows a time trace of this user's throughput from frames 400-600.

The lower plot shows the MS's predicted ASINR (representative of the ESINR used by the fast AMC algorithm) alongside the actual ASINR the MS experiences. The predicted ASINR is taken from the 3-frame delayed CQI. The predicted (stars), and actual (crosses), ASIRs appear directly on top of these lines showing that the MS is interference limited. Moving to the middle plot, we see the corresponding current MCS choice (solid line) and ideal MCS choice (dashed). This then translates (in the upper plot) to the actual frame throughput (solid line) and the ideal frame throughput (dashed line) based on the ideal MCS choice for the current frame.

There are many regions where the ideal throughput surpasses the actual throughput. Just before frame 480, the predicted ASINR climbs and so MCS mode 6 is chosen by the AMC algorithm. The actual ASINR in this frame is significantly lower than predicted so the BLER rises and the throughput falls to zero. The ideal case shows that if MCS mode 6 had been chosen earlier, higher throughput could have been achieved as this high mode would have coincided with the ASINR peak. Clearly, the variation of ASINR is dominated by the large ASIR fluctuation and not by the much smaller ASNR fluctuation. In this small section, where the ASNR is consistently high, a potential improvement in the average throughput from 109 up to 159kbps could be achieved with better interference management.

On the UL, MS 0.1 experienced an 11.5% increase in throughput (113kbps-126kbps) when ideal MCS choices were used instead of those based on a 3-frame delayed CQI. For a 1-frame CQI delay the throughput was 117kbps. On the DL the greatest improvement over a 3-frame delayed CQI was user MS 2.4 at 48.8%. On the UL, MS 2.0 saw an improvement of 22%.

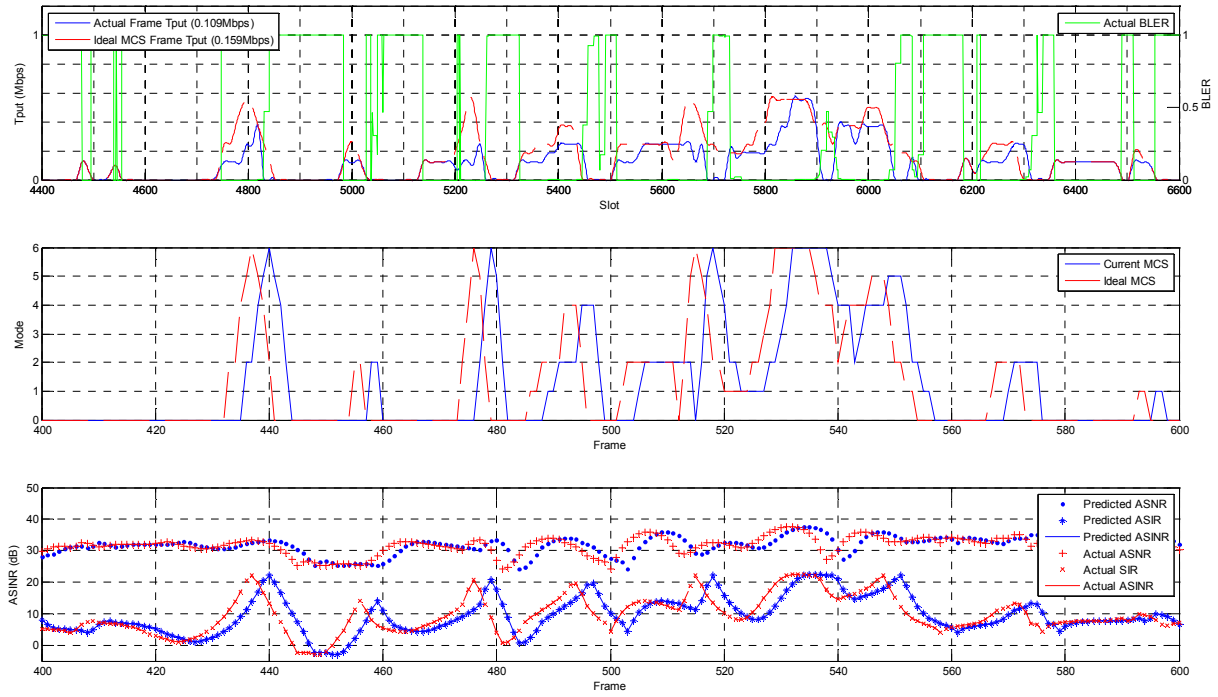


Figure 4. MS 2.0 DL performance, frames 400-600

## V. CONCLUSIONS

This paper has discussed the architecture and algorithms required to develop a detailed and efficient OFDMA based system level simulator. The simulator is able to provide deep insights into complex issues such as inter-cell interference and MCS mode selection on both the UL and DL.

In interference limited situations it was shown that the fluctuation in interference power dominates the inaccuracies seen in the predicted CQI. This information is used by the fast AMC algorithm to select the MCS mode in a future frame and choice of the incorrect MCS mode was seen to cause a reduction in throughput. Using the ideal MCS mode per frame, rather than that derived from the 3-frame delayed CQI, improved throughput by up to 48.8% on the DL and 22% on the UL. The use of subcarrier permutation was shown to help reduce the variance of both the SNR and SIR. Using a different permutation sequence for different BSs was seen to further reduce the SIR variance (on the UL only).

This work highlights the necessity for detailed interference characterization and management in OFDMA based networks. Although the simulator is based on mobile WiMAX, its algorithms and methods can easily be extended to other mobile broadband wireless networks, such as LTE.

## ACKNOWLEDGMENTS

The authors would like to thank Dr Mai Tran for his work on the OFDMA link-level simulator. David Halls would also like to that the UK EPSRC and Motorola for their kind financial assistance and Lorenz Freiberg of Motorola for his technical input.

## REFERENCES

[1] "IEEE Std 802.16e-2005 and IEEE Std 802.16-2004/Cor 1-2005," 2006.

[2] G. Boudreau, J. Panicker, N. Guo, R. Chang, N. Wang, and S. Vrzic, "Interference coordination and cancellation for 4G networks - [LTE part II: 3GPP release 8]," *IEEE Communications Magazine*, vol. 47, pp. 74-81, 2009.

[3] A. V. Sarad and S. Srikanth, "Improved interference diversity in multicellular OFDMA systems," *COMSNETS,* pp. 1-8, Jan. 2009.

[4] M. Hunukumbure, B. Upase, and S. Vadgama, "Modelling interference margins in FFR enabled WiMAX systems for cell dimensioning," *IEEE PIMRC*, pp. 1-5, Sept, 2008.

[5] B. J. Lee, J. W. Kim, J. C. Kim, and C. G. Kang, "System-level Performance of MIMO-based Mobile WiMAX System," *IEEE MWS*, pp. 189-194, July 2009.

[6] M. Shariat, A. Ul Quddus, and R. Tafazolli, "On the efficiency of interference coordination schemes in emerging cellular wireless networks," *IEEE PIMRC*, pp. 1-5, Sept 2008.

[7] A. L. Stolyar and H. Viswanathan, "Self-Organizing Dynamic Fractional Frequency Reuse for Best-Effort Traffic through Distributed Inter-Cell Coordination," *IEEE INFOCOM*, pp. 1287-1295, April 2009.

[8] S. Hamouda, C. Yeh, J. Kim, S. Wooram, and D. S. Kwon, "Dynamic hard Fractional Frequency Reuse for mobile WiMAX,". *IEEE PerCom*, pp. 1-6, March 2009.

[9] J. Zhuang, L. Jalloul, R. Novak, and J. Park, "IEEE 802.16m Evaluation Methodology Document," 2009.

[10] Y. Q. Bian, A. R. Nix, E. K. Tameh, and J. P. McGeehan, "MIMO-OFDM WLAN Architectures, Area Coverage, and Link Adaptation for Urban Hotspots," *IEEE Transactions on Vehicular Technology*, vol. 57, No. 4, pp. 2364-2374, 2008.

[11] Z. Wang, E. K. Tameh, and A. R. Nix, "Joint Shadowing Process in Urban Peer-to-Peer Radio Channels," *IEEE Transactions on Vehicular Technology*, vol. 57, No. 1, pp. 52-64, 2008.

[12] M. Tran, D. Halls, A. Nix, A. Doufexi, and M. Beach, "Mobile WiMAX: MIMO Performance Analysis from a Quality of Service (QoS) Viewpoint," *IEEE WCNC,* pp. 1-6, April 2009.

[13] L. Wan, S. Tsai, and M. Almgren, "A fading-insensitive performance metric for a unified link quality model," *IEEE WCNC,* pp. 2210-2114, April 2006.

[14] M. K. Karray, "Electromagnetic Exposure and Quality of Service in the Downlink of Wireless Cellular Networks," *ICWMC*, Sept. 2010.